Supplementary Information

Synergistic absorbents based on $SnFe_2O_4$@ZnO nanoparticles decorated with reduced graphene oxide for highly efficient dye adsorption at room temperature

Pawan Kumar Singh[1], Kuan-Yi Kuo,[a] Jui-Teng Lee[1], Po-Hsuan Hsiao[1], Joon Ching Juan[2], Hong Phan Duong[3], and Chia-Yun Chen[1,4*]

[1]Department of Materials Science and Engineering, National Cheng Kung University, Tainan 70101, Taiwan

[2]Nanotechnology & Catalysis Research Centre, Institute for Advanced Studies, University of Malaya, 50603 Kuala Lumpur, Malaysia

[3]The University of Danang, University of Science and Technology, 54 Nguyen Luong Bang, Vietnam

[4]Hierarchical Green-Energy Materials (Hi-GEM) Research Center, National Cheng Kung University, Tainan

S1 Synthetic parameters, SEM, XRD and XPS results of $SnFe_2O_4$ nanoparticles

The co-precipitation method was employed for the formation of $SnFe_2O_4$ nanoparticles, where the involved chemical reaction is shown below,

$$Sn^{2+} + Fe^{3+} + 8OH^- \rightarrow SnFe_2O_4 + 4H_2O \quad (1)$$

The detailed synthetic parameters are presented in Table S1. Figs. S1 shows the morphologies of five various nanoparticles, which indicates that the nanoparticle sizes can be turned with the control of precursor concentrations. The corresponding XRD patterns are demonstrated in Fig. S1(f), where the peaks at 2θ of 30.2°,35.6° ,44.09°, 53.3°, 62.6° are correlated with the (220), (311), (400), (422), (440) of spinel $SnFe_2O_4$ crystals. In the adsorption experiment, the synthetic condition of $SnFe_2O_4$-IV is adopted due to the existence of uniform size distributions. In addition, XPS results of synthesized $SnFe_2O_4$/ZnO@rGO nanocomposites are presented in Fig. S2.

Table S1 Synthetic parameters of $SnFe_2O_4$ nanoparticles.

Sample	$W_{SnCl_2(S)}$ **(mg)**	$W_{Fe(NO_3)_3 \cdot 9H_2O(S)}$ **(mg)**	$\mathbf{V}_{\mathbf{ethanol}}$ **(ml)**
$SnFe_2O_4$-I	**11.1**	**47.3**	**10**

$SnFe_2O_4$-IV	**22.2**	**94.6**	**10**
$SnFe_2O_4$-III	**44.4**	**189.2**	**10**
$SnFe_2O_4$-IV	**88.9**	**378.8**	**10**
$SnFe_2O_4$-V	**133.3**	**568.1**	**10**

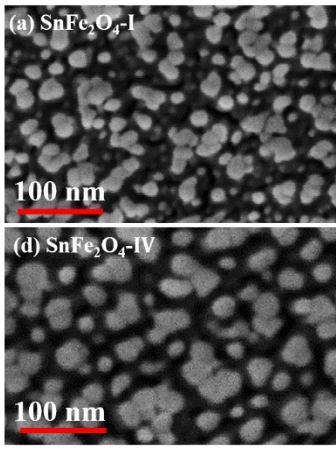

Fig. S1 (a)-(e) SEM images of various $SnFe_2O_4$ samples and (f) the corresponding XRD patterns.

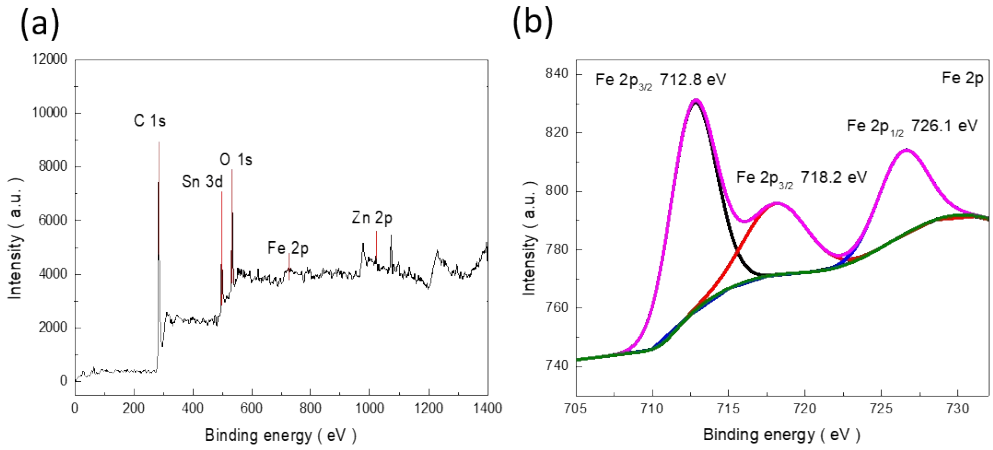

Fig. S2 XPS analysis of $SnFe_2O_4$@ZnO@rGO nanocomposites. Fig. S2(a) indicates that the existence of peaks corresponding to C 1s, Sn 3d, O 1s, Fe 2p, Zn 2p, respectively. In addition, the peaks located at 712.8 eV and 718.2 are attributed to the spin–orbit splitting of the Fe $2p_{3/2}$, and the additional peak at 726.1 eV is assigned to be the spin–orbit splitting of the Fe $2p_{1/2}$.

S2 Measurements of magnetization hysteresis loops

Fig S3 shows the magnetic hysteresis loops of the sole $SnFe_2O_4$ nanoparticles (black line) and $SnFe_2O_4$@ZnO@rGO (16 wt%) nanocomposites (red line) at room

temperature measured under an applied magnetic field sweeping from -10 to 10 k Oe, where all the resulting hysteresis loops demonstrate the typical S-like curves. Moreover, the saturation magnetization (M_s) of $SnFe_2O_4$ and $SnFe_2O_4$/ZnO@rGO nanocomposites are comparable, with the values of 15.3 emu/g and 13.5 emu/g, respectively, as presented in the inset of Fig. S2. In addition, the used nanocomposites can be collected quickly by using an external magnet, and employed for repeated adsorption of organic dyes.

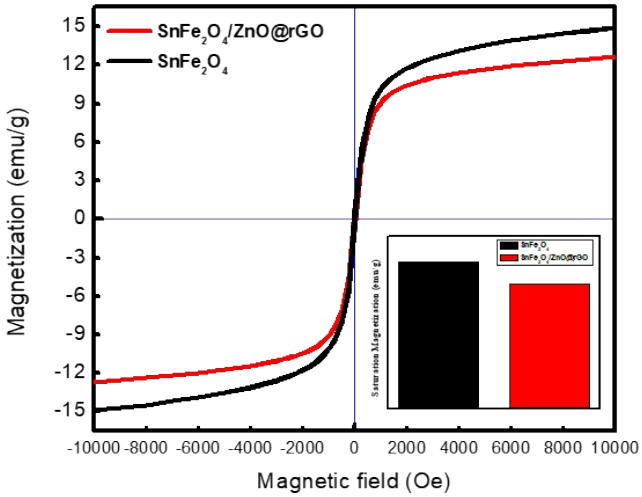

Fig S3 Magnetic hysteresis loops of the $SnFe_2O_4$ nanoparticles (black line) and $SnFe_2O_4$/ZnO@rGO nanocomposites (red line) at room temperature.

S3 Photoluminescence spectra of various samples

Fig. S4 shows the photoluminescence (PL) spectra of $SnFe_2O_4$/ZnO and $SnFe_2O_4$/ZnO@rGO nanocomposites, respectively. The almost consistent PL spectra can be found with central emission peak located at 530 nm, which is originated from the point defects from the vacant O^{2-} sites of involved ZnO seeds.

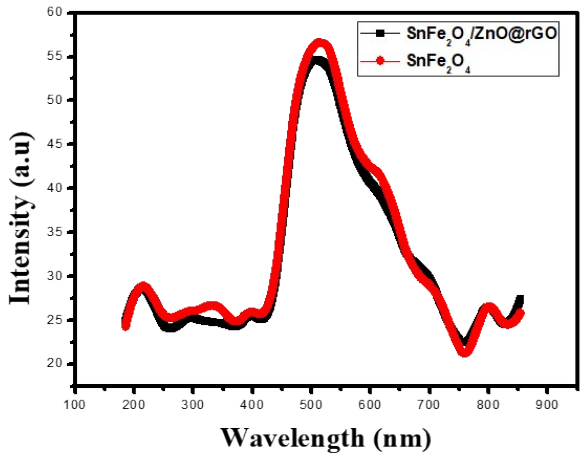

Fig. S4 PL spectra of $SnFe_2O_4$/ZnO and $SnFe_2O_4$/ZnO@rGO nanocomposites.

S4 N_2 adsorption-desorption isotherms of various samples

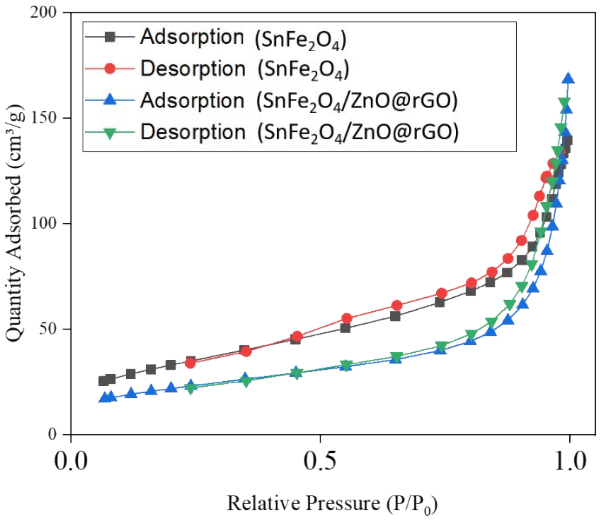

Fig. S5 (a) N_2 adsorption-desorption isotherms of $SnFe_2O_4$ nanoparticles and $SnFe_2O_4$/ZnO@rGO nanocomposites, respectively.

S5 Effects of pH conditions on dye adsorption

Variations of pH value in the tested dye solutions are a critical issue regarding the practical applications of adsorbents. From Fig. S5, one can find that the dye adsorption efficiencies using $SnFe_2O_4$/ZnO@rGO nanocomposites reach the sound values ranging from 79.6% to 92.8% while pH conditions are varied from 3 to 11.

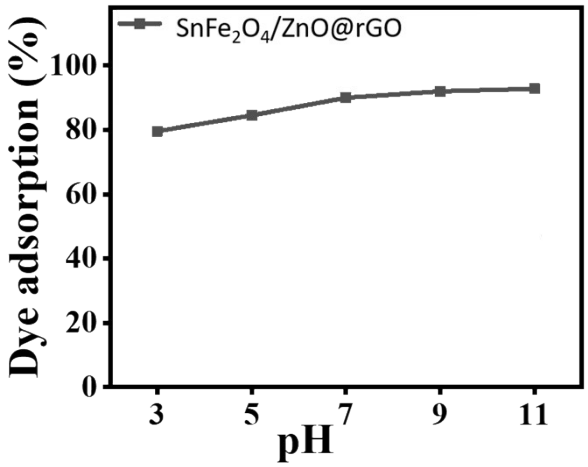

Fig. S6 Dye adsorption results of $SnFe_2O_4$/ZnO@rGO nanocomposites in the presence of MB dyes under various pH conditions.

S6 Effects of concentrations and types of dyes on adsorption capability

Fig. S7(a) shows the adsorption performance of designed adsorbents as $SnFe_2O_4$/ZnO@rGO nanocomposites under wide range of MB concentrations from 0.001 mM to 0.007 mM, where the results indicate no clear saturation in the presence of high concentrated dyes. In addition, Fig. S7(b) presents the adsorption capabilities of $SnFe_2O_4$/ZnO@rGO nanocomposites in the presence of mixed cationic dyes, including MB, RhB and R6G dyes and anionic dyes, including MO and RB5 dyes, respectively.

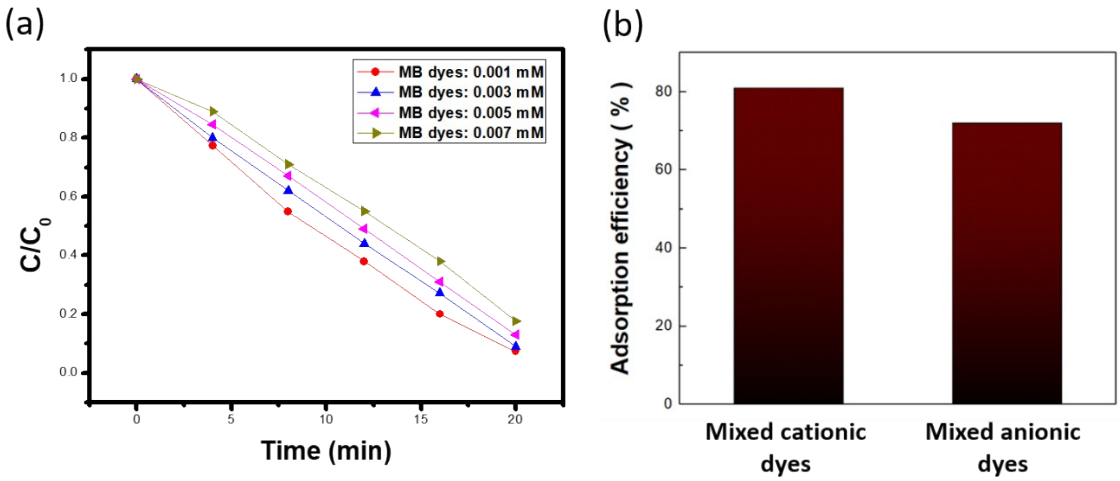

Fig. S7 Adsorption efficiency of $SnFe_2O_4$/ZnO@rGO nanocomposites (a) under various concentrations of MB dyes and (b) in the presence of mixed cationic dyes, anionic dyes, respectively.